36th Hampton University Graduate Studies Program (*e*-HUGS 2021)

Momentum Tomography of Light Mesons

Satvir Kaur

Dr. B.R. Ambedkar National Institute of Technology, Jalandhar, India

June 17, 2021

Overview

The study of Hadron Physics aims to understand the nature of the matter that we observe in the universe.

Hadron Tomography

- The complex internal structure of the hadron can be studied by choosing the different high energy processes.
- Different processes are accessible at different energy scales.
- The two energy scale regimes are convoluted in the cross section as:
  - the partonic cross-section (calculable with the perturbative methods)
  - the nonperturbative part.

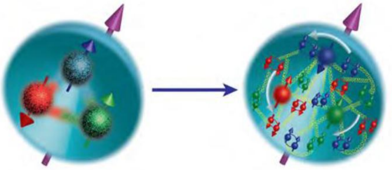

[1]

- One of the possible approaches used to study the nonperturbative aspects is based on the light-front Hamiltonian approach [2].

[1] D. G. Ireland

[2] S. J. Brodsky, H.-C Pauli, and S. S. Pinsky, Phys. Rept. 301, 299 (1998).

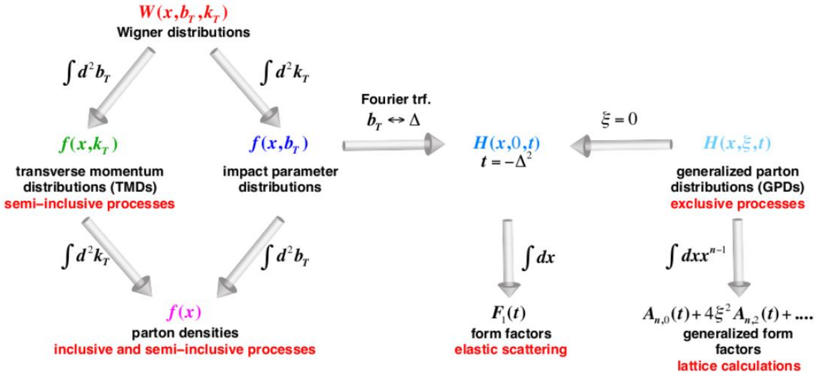

[1]

–briefly explained by Andrea Signori

[1] A. Accardi *et al.*, Eur.Phys.J.A 52 (2016) 9, 268.

Light-Front Dynamics

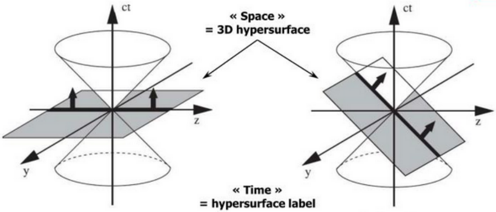

Equal t		Equal τ
p^0	$\leftrightarrow$	$p^- = p^0 - p^3$
(p^1, p^2)	$\leftrightarrow$	$\vec{p}_\perp$
p^3	$\leftrightarrow$	$p^+ = p^0 + p^3$

[0] P. A. M. Dirac, Rev. Mod. Phys. 21, 392 (1949).

[0] S. J. Brodsky, G. F. de Teramond, Phys. Rev. D 77, 056007 (2008).

Light-Front Dynamics

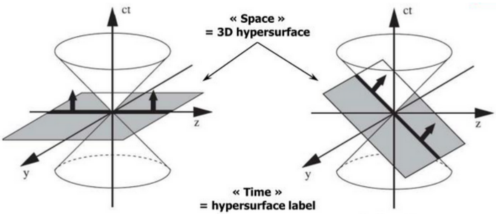

Equal t		*Equal τ*
p^0	$\Leftrightarrow$	$p^- = p^0 - p^3$
(p^1, p^2)	$\Leftrightarrow$	$\vec{p}_\perp$
p^3	$\Leftrightarrow$	$p^+ = p^0 + p^3$

Light-front provides the wavefunctions (LFWFs) encode the hadronic properties in terms of their quark and gluon degrees of freedom.

[0] P. A. M. Dirac, Rev. Mod. Phys. 21, 392 (1949).

[0] S. J. Brodsky, G. F. de Teramond, Phys. Rev. D 77, 056007 (2008).

Light-Front Holographic QCD

- Holographic methods allows one to map the functional dependence of AdS wavefunctions to the holographic wavefunctions in physical space-time.
- The transverse part of the wavefunction satisfies the holographic Schrödinger Equation:

$$\left(-\frac{\mathrm{d}^2}{\mathrm{d}\zeta^2} - \frac{4L^2-1}{4\zeta^2} + U(\zeta)\right)\Phi(\zeta) = M^2\Phi(\zeta)$$

where $\zeta = \sqrt{x(1-x)}b_\perp$

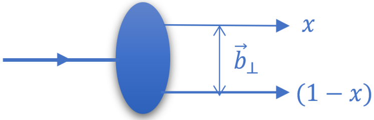

- The complete meson wavefunction is given by [1]

$$\varphi_{nL}(x,\zeta,\theta) = \frac{\Phi_{nL}(\zeta)}{\sqrt{2\pi\zeta}}X(x)e^{iL\theta}$$

[1] S. J. Brodsky, G. F. de Téramond, H. G. Dosch, and J. Erlich, Phys. Rept. 584, 1 (2015).

- In momentum space, the holographic wavefunction becomes:

$$\varphi^{\mathrm{LFH}}(x, k_\perp^2) \propto \frac{1}{\sqrt{x\bar{x}}} \exp\left(-\frac{k_\perp^2}{2\kappa^2 x\bar{x}}\right) \exp\left(-\frac{1}{2\kappa^2}\left(\frac{m_f^2}{x} + \frac{m_{\bar{f}'}^2}{\bar{x}}\right)\right)$$

No difference between the pseudoscalar and vector meson wavefunctions.

No quark/antiquark helicities included till now.

- Dynamical spin effects were included [2] [3].

[1] S. J. Brodsky and G. F. de Téramond, Subnucl. Ser. 45, 139 (2009).

[2] M. Ahmady, C. Mondal, and R. Sandapen, Phys. Rev. D98, 034010 (2018); M. Ahmady, F. Chishtie, and R. Sandapen, Phys. Rev. D95, 074008 (2017).

[3] J. R. Forshaw and R. Sandapen, Phys. Rev. Lett. 109, 081601 (2012); M. Ahmady and R. Sandapen, Phys. Rev. D88, 014042 (2013).

- In momentum space, the holographic wavefunction becomes:
- A prescription by Brodsky *et al.*[1]

$$\varphi^{\mathrm{LFH}}(x, k_\perp^2) \propto \frac{1}{\sqrt{x\bar{x}}} \exp\left(-\frac{k_\perp^2}{2\kappa^2 x\bar{x}}\right) \exp\left(-\frac{1}{2\kappa^2}\left(\frac{m_f^2}{x} + \frac{m_{\bar{f}'}^2}{\bar{x}}\right)\right)$$

No difference between the pseudoscalar and vector meson wavefunctions.

No quark/antiquark helicities included till now.

- Dynamical spin effects were included [2] [3].

[1] S. J. Brodsky and G. F. de Téramond, Subnucl. Ser. 45, 139 (2009).

[2] M. Ahmady, C. Mondal, and R. Sandapen, Phys. Rev. D98, 034010 (2018); M. Ahmady, F. Chishtie, and R. Sandapen, Phys. Rev. D95, 074008 (2017).

[3] J. R. Forshaw and R. Sandapen, Phys. Rev. Lett. 109, 081601 (2012); M. Ahmady and R. Sandapen, Phys. Rev. D88, 014042 (2013).

- In momentum space, the holographic wavefunction becomes:
- A prescription by Brodsky *et al.*[1]

$$\varphi^{\mathrm{LFH}}(x, k_\perp^2) \propto \frac{1}{\sqrt{x\bar{x}}} \exp\left(-\frac{k_\perp^2}{2\kappa^2 x\bar{x}}\right) \exp\left(-\frac{1}{2\kappa^2}\left(\frac{m_f^2}{x} + \frac{m_{\bar{f}'}^2}{\bar{x}}\right)\right)$$

No difference between the pseudoscalar and vector meson wavefunctions.

No quark/antiquark helicities included till now.

- Dynamical spin effects were included [2] [3].

[1] S. J. Brodsky and G. F. de Téramond, Subnucl. Ser. 45, 139 (2009).

[2] M. Ahmady, C. Mondal, and R. Sandapen, Phys. Rev. D98, 034010 (2018); M. Ahmady, F. Chishtie, and R. Sandapen, Phys. Rev. D95, 074008 (2017).

[3] J. R. Forshaw and R. Sandapen, Phys. Rev. Lett. 109, 081601 (2012); M. Ahmady and R. Sandapen, Phys. Rev. D88, 014042 (2013).

- In momentum space, the holographic wavefunction becomes:
- A prescription by Brodsky *et al.*[1]

$$\varphi^{\mathrm{LFH}}(x, k_\perp^2) \propto \frac{1}{\sqrt{x\bar{x}}} \exp\left(-\frac{k_\perp^2}{2\kappa^2 x\bar{x}}\right) \exp\left(-\frac{1}{2\kappa^2}\left(\frac{m_f^2}{x} + \frac{m_{\bar{f}'}^2}{\bar{x}}\right)\right)$$

No difference between the pseudoscalar and vector meson wavefunctions.

No quark/antiquark helicities included till now.

- Dynamical spin effects were included [2] [3].

[1] S. J. Brodsky and G. F. de Téramond, Subnucl. Ser. 45, 139 (2009).

[2] M. Ahmady, C. Mondal, and R. Sandapen, Phys. Rev. D98, 034010 (2018); M. Ahmady, F. Chishtie, and R. Sandapen, Phys. Rev. D95, 074008 (2017).

[3] J. R. Forshaw and R. Sandapen, Phys. Rev. Lett. 109, 081601 (2012); M. Ahmady and R. Sandapen, Phys. Rev. D88, 014042 (2013).

- In momentum space, the holographic wavefunction becomes:
- A prescription by Brodsky *et al.*[1]

$$\varphi^{\mathrm{LFH}}(x,k_\perp^2) \propto \frac{1}{\sqrt{x\bar{x}}} \exp\left(-\frac{k_\perp^2}{2\kappa^2 x\bar{x}}\right) \exp\left(-\frac{1}{2\kappa^2}\left(\frac{m_f^2}{x}+\frac{m_{\bar{f}'}^2}{\bar{x}}\right)\right)$$

No difference between the pseudoscalar and vector meson wavefunctions.

No quark/antiquark helicities included till now.

- Dynamical spin effects were included [2] [3].

[1] S. J. Brodsky and G. F. de Téramond, Subnucl. Ser. 45, 139 (2009).

[2] M. Ahmady, C. Mondal, and R. Sandapen, Phys. Rev. D98, 034010 (2018); M. Ahmady, F. Chishtie, and R. Sandapen, Phys. Rev. D95, 074008 (2017).

[3] J. R. Forshaw and R. Sandapen, Phys. Rev. Lett. 109, 081601 (2012); M. Ahmady and R. Sandapen, Phys. Rev. D88, 014042 (2013).

Momentum Tomography of Hadrons

To get the information of hadron structure in momentum space, TMDs$(x, \mathbf{k}_\perp^2)$ were introduced.

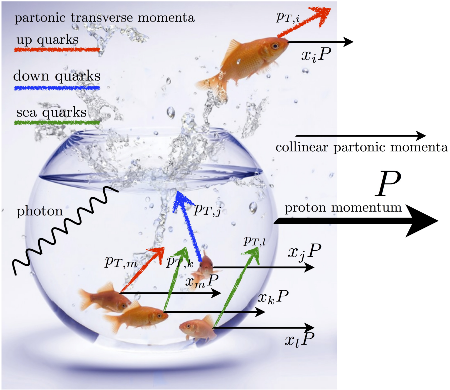

[1] Andrea Signori

Spin-1 hadron

S. Kaur, C. Mondal and H. Dahiya,
"Light-front holographic ρ-meson distributions in the momentum space,"
JHEP 01, 136 (2021)

TMDs

leading twist		quark operator		
		unpolarized [U]	longitudinal [L]	transverse [T]
target polarization	U	$f_1 =$ unpolarized		$h_1^\perp = \ -$ Boer-Mulders
	L		$g_1 = \ -$ helicity	$h_{1L}^\perp = \ -$ worm gear 1
	T	$f_{1T}^\perp = \ -$ Sivers	$g_{1T} = \ -$ worm gear 2	$h_1 = \ -$ transversity $h_{1T}^\perp = \ -$ pretzelosity
	TENSOR	$\theta_{LL}(x, \boldsymbol{k}_T^2)$ $\theta_{TT}(x, \boldsymbol{k}_T^2)$ $\theta_{LT}(x, \boldsymbol{k}_T^2)$	$g_{1TT}(x, \boldsymbol{k}_T^2)$ $g_{1LT}(x, \boldsymbol{k}_T^2)$	$h_{1LL}^\perp(x, \boldsymbol{k}_T^2)$ h_{1TT}, $h_{1TT}^\perp$ h_{1LT}, $h_{1LT}^\perp$

[1] Here, $\theta = f$.

- 9 T-even and 9 T-odd TMDs including tensor polarized TMDs.
- For spin-1 hadron, there exists the tensor structure, which is absent in case of spin<1.

- Tensor polarized structures are related to the unpolarized quark distribution in the polarized spin-1 hadron.

[1] Ian Cloët

- The $\mathbf{k}_\perp$-dependent quark-quark correlator:

$$\Theta_{ij}^{(\Lambda)\mathbf{S}}(x,\mathbf{k}_\perp) = \int \frac{\mathrm{d}z^-\,\mathrm{d}^2\mathbf{z}_\perp}{(2\pi)^3}\, e^{\iota k\cdot z}\,{}_\Lambda\langle P,S|\bar{\vartheta}_j(0)\vartheta_i(z^-,\mathbf{z}_\perp)|P,S\rangle_\Lambda|_{z^+=0}$$

$$\langle\Gamma\rangle_{\mathcal{S}}^{(\Lambda)} = \frac{1}{2}\mathrm{Tr}_D\left(\Gamma\Theta^{(\Lambda)\mathcal{S}}\right)$$

- At the leading-twist,

$$\langle\gamma^+\rangle_{\mathbf{S}}^{(\Lambda)}(x,\mathbf{k}_\perp^2) = f_1 - \frac{3\Lambda^2-2}{2}\left(\left(S_L^2-\frac{1}{3}\right)f_{1LL} + S_L\frac{\mathbf{k}_\perp\cdot\mathbf{S}_T}{M_H}f_{1LT} + \frac{(\mathbf{k}_\perp\cdot\mathbf{S}_T)^2-\frac{1}{3}k_\perp^2}{M_H^2}f_{1TT}\right);$$

$$\langle\gamma^+\gamma_5\rangle_{\mathbf{S}}^{(\Lambda)}(x,\mathbf{k}_\perp^2) = \ \ldots \qquad ; \qquad \langle\gamma^+\gamma^i\gamma_5\rangle_{\mathbf{S}}^{(\Lambda)}(x,\mathbf{k}_\perp^2) = \ \ldots$$

(a) Unpolarized

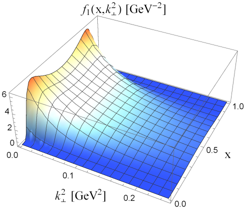

(b) Helicity

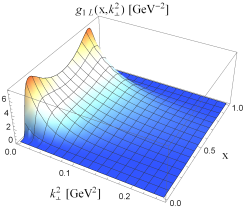

(c) Worm gear 2

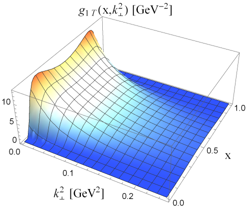

(d) Worm gear 1

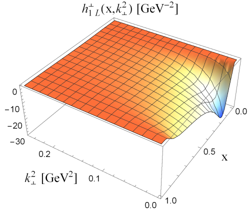

(e) Transversity

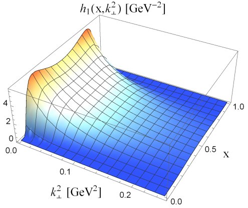

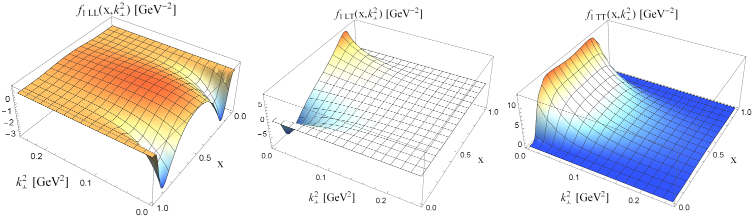

- f_1, g_{1L}, h_1 and f_{1LL} are diagonal in the OAM. The overlap configurations of the other TMDs show interference between several wave compositions.
- The S-wave contribution dominates at the central region of x, where f_{1LL} vanishes, whereas at lower and higher x domains, the other contributions rule over i.e. $L \geq 1$.
- f_{1LT} can be observed by polarizing the spin-1 hadron with angles 45° and 135° with respect to the hadron momentum direction [1].
- f_{1LL} and f_{1LT} got vanished at $x = 1/2$ for all $\mathbf{k}_\perp^2$, which means the relative momentum between the valence constituents is zero.

[1] S. Hino and S. Kumano, Phys. Rev. D 59, 094026 (1999).

Parton Distribution Functions (PDFs)

- Integrating the TMDs over $\mathbf{k}_\perp$ lead to leading twist PDFs: $f_1(x)$, $g_1(x)$, $h_1(x)$ and $f_{1LL}(x)$.
- The tensor polarized PDF is defined as:

$$f_{1LL}(x) \propto \left(q^0(x) - \frac{q^{+1}(x) + q^{-1}(x)}{2} \right)$$

- In literature, the tensor polarized distribution exists as $b_1(x)$.
- Experimentally, it can be determined by measuring the deep inelastic cross section for an unpolarized lepton beam to scatter from a polarized target along the beam and subtracting this cross section for an unpolarized target [1].
- The experimental data of $b_1(x)$ has been already taken by HERMES for the deuteron case [2].
- A proposal was approved to measure b_1 at JLab. Much progress is expected for b_1 in the near future [3] [4].
- The tensor structure studies in terms of quark and gluon degrees of freedom, different from ordinary descriptions, could open a new era of high-energy spin physics.

[1] P. Hoodbhoy, R. L. Jaffe and A. Manohar, Nucl. Phys. B 312, 571 (1989).

[2] HERMES Collaboration, A. Airapetian *et al.*, Phys. Rev. Lett. 95, 242001 (2005).

[3] K. Slifer, J. Phys. Conf. Ser. 543, 012003 (2014).

[4] Jefferson Lab experiment E12-13-011.

- We investigated the valence quark PDFs in case of ρ meson using light-front inspired models.
- At the model scale, the sum rules are satisfied by our PDFs [3]:

$$\int_0^1 \mathrm{d}x \; f_1(x) = 1$$

$$\int_0^1 \mathrm{d}x \; x \; f_1(x) + \int_0^1 \mathrm{d}x \; (1-x) \; f_1(x) = 1$$

$$\int_0^1 \mathrm{d}x \; f_{1LL}(x) = 0 \; ; \int_0^1 \mathrm{d}x \; x \; f_{1LL}(x) = 0$$

- The positivity conditions for quark PDFs in case of spin-1 hadron [2]:

$$f_1(x) \geq 0 \quad ; \quad 3f_1(x) \geq f_{1LL}(x) \geq -\frac{3}{2} f_1(x)$$

$$\frac{3}{2} f_1(x) \geq f_1(x) - \frac{1}{3} f_{1LL}(x) \geq |g_1(x)|$$

$$\left(f_1(x) + \frac{2}{3} f_{1LL}(x)\right)\left(f_1(x) + g_1(x) - \frac{1}{3} f_{1LL}(x)\right) \geq 2|h_1(x)|^2$$

[1] Y. Ninomiya, W. Bentz and I. C. Cloët, Phys. Rev. C 96, 045206 (2017).
[2] A. Bacchetta and P. J. Mulders, Phys. Lett. B 518, 85 (2001).

- We investigated the valence quark PDFs in case of ρ meson using light-front inspired models.
- At the model scale, the sum rules are satisfied by our PDFs [3]:

$$\int_0^1 \mathrm{d}x \; f_1(x) = 1$$

$$\int_0^1 \mathrm{d}x \; x \; f_1(x) + \int_0^1 \mathrm{d}x \; (1-x) \; f_1(x) = 1$$

$$\int_0^1 \mathrm{d}x \; f_{1LL}(x) = 0 \, ; \int_0^1 \mathrm{d}x \; x \; f_{1LL}(x) = 0$$

- The positivity conditions for quark PDFs in case of spin-1 hadron [2]:

$$f_1(x) \geq 0 \quad ; \quad 3f_1(x) \geq f_{1LL}(x) \geq -\frac{3}{2} f_1(x)$$

$$\frac{3}{2} f_1(x) \geq f_1(x) - \frac{1}{3} f_{1LL}(x) \geq |g_1(x)|$$

$$\left(f_1(x) + \frac{2}{3} f_{1LL}(x)\right)\left(f_1(x) + g_1(x) - \frac{1}{3} f_{1LL}(x)\right) \geq 2|h_1(x)|^2$$

[1] Y. Ninomiya, W. Bentz and I. C. Cloët, Phys. Rev. C 96, 045206 (2017).
[2] A. Bacchetta and P. J. Mulders, Phys. Lett. B 518, 85 (2001).

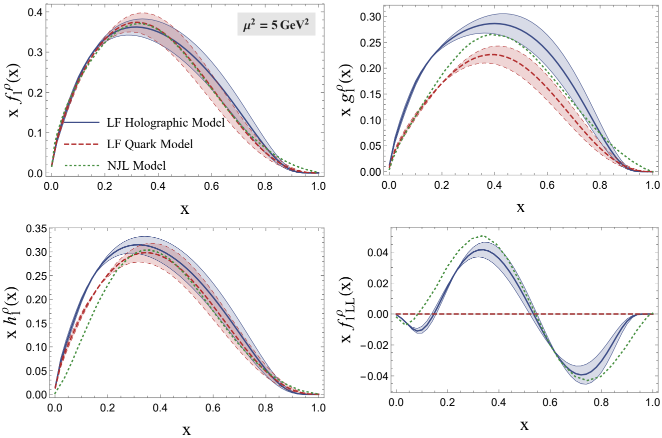

[1] Y. Ninomiya, W. Bentz and I. C. Cloët, Phys. Rev. C 96, 045206 (2017).

Spin-0 hadron

S. Kaur, N. Kumar, J. Lan, C. Mondal and H. Dahiya,
"Tomography of light mesons in the light-cone quark model"
Phys. Rev. D ***102****, 014021 (2020).*

TMDs

$$\langle\gamma^+\rangle(x,\mathbf{k}_\perp^2) \equiv f_1^{\mathcal{P}}(x,\mathbf{k}_\perp^2)$$

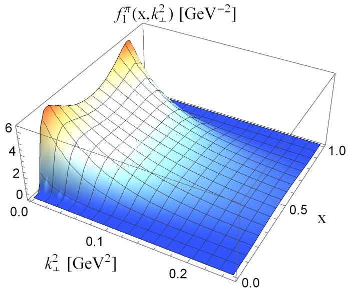

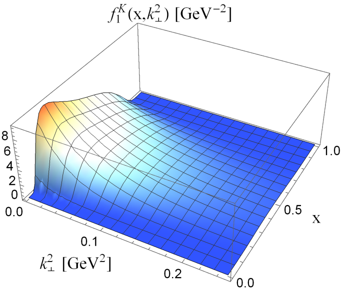

[1]

[1] M. Ahmady, C. Mondal and R. Sandapen, Phys. Rev. D 100, 054005 (2019)

$$\langle \iota\sigma^{i+}\gamma_5\rangle(x,\mathbf{k}_\perp^2) \equiv \frac{\epsilon^{ij}k_\perp^j}{M_{\mathcal{P}}} h_1^{\perp\mathcal{P}}(x,\mathbf{k}_\perp^2)$$

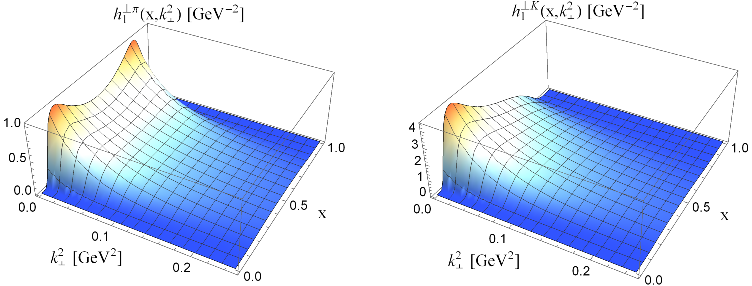

[1]

[1] M. Ahmady, C. Mondal and R. Sandapen, Phys. Rev. D 100, 054005 (2019)

PDFs

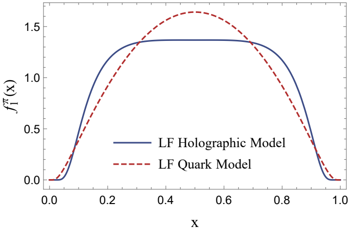

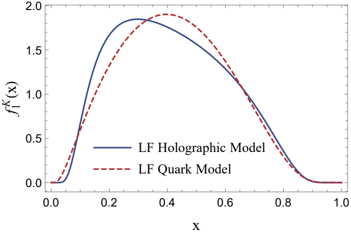

[1] J. S. Conway et al. (E615 Collaboration), Phys. Rev. D 39, 92 (1989).
[2] M. Aicher, A. Schafer and W. Vogelsang, Phys. Rev. Lett. 105, 252003 (2010).
[3] J. Lan, C. Mondal, S. Jia, X. Zhao, J. P. Vary, Phys. Rev. Lett. 122, 172001 (2019).
[4] M. Ahmady, C. Mondal and R. Sandapen, Phys. Rev. D 98, 034010 (2018).

PDFs

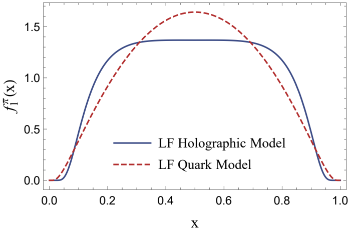

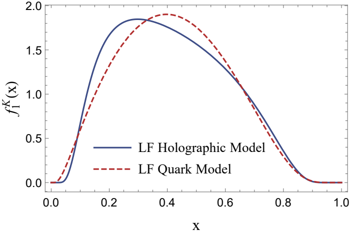

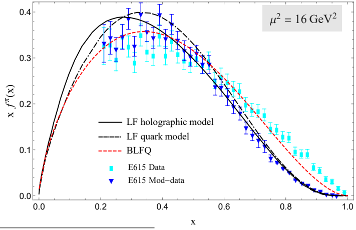

[1] J. S. Conway et al. (E615 Collaboration), Phys. Rev. D 39, 92 (1989).
[2] M. Aicher, A. Schafer and W. Vogelsang, Phys. Rev. Lett. 105, 252003 (2010).
[3] J. Lan, C. Mondal, S. Jia, X. Zhao, J. P. Vary, Phys. Rev. Lett. 122, 172001 (2019).
[4] M. Ahmady, C. Mondal and R. Sandapen, Phys. Rev. D 98, 034010 (2018).

Summary

ρ-meson

- Investigated various T-even TMDs: there are total 9 T-even TMDs, from which 8 are non-zero in LF holographic model.
- Our findings of the valence quark TMDs and PDFs found to be consistent with the NJL model results and also have satisfied all the positivity conditions.
- The presented results in this study together with other theoretical predictions on the TMDs and the PDFs may help the experimental groups to measure these distributions for the ρ-meson.

Summary

ρ-meson

- Investigated various T-even TMDs: there are total 9 T-even TMDs, from which 8 are non-zero in LF holographic model.
- Our findings of the valence quark TMDs and PDFs found to be consistent with the NJL model results and also have satisfied all the positivity conditions.
- The presented results in this study together with other theoretical predictions on the TMDs and the PDFs may help the experimental groups to measure these distributions for the ρ-meson.

Pseudoscalar mesons

- Showed the TMDs: the unpolarized $f_1(x, \mathbf{k}_\perp^2)$ and Boer-Mulder's $h_1^\perp(x, \mathbf{k}_\perp^2)$.
- Investigated the only non-zero PDF $f_1(x)$ for pseudoscalar mesons. For pion case, we found excellent agreement with modified E615 data after applying QCD evolution.

Summary

ρ-meson

- Investigated various T-even TMDs: there are total 9 T-even TMDs, from which 8 are non-zero in LF holographic model.
- Our findings of the valence quark TMDs and PDFs found to be consistent with the NJL model results and also have satisfied all the positivity conditions.
- The presented results in this study together with other theoretical predictions on the TMDs and the PDFs may help the experimental groups to measure these distributions for the ρ-meson.

Pseudoscalar mesons

- Showed the TMDs: the unpolarized $f_1(x, \mathbf{k}_\perp^2)$ and Boer-Mulder's $h_1^\perp(x, \mathbf{k}_\perp^2)$.
- Investigated the only non-zero PDF $f_1(x)$ for pseudoscalar mesons. For pion case, we found excellent agreement with modified E615 data after applying QCD evolution.

Thanks